

# Electrochemical control of heterolytic and homolytic hydrogenation pathways at a palladium surface

Mia D. Stankovic,<sup>1</sup> Bowen Ge,<sup>1</sup> Jessica F. Sperry,<sup>1</sup> and Curtis P. Berlinguette<sup>1,2,3,4,\*</sup>

<sup>1</sup>Department of Chemistry, The University of British Columbia, 2036 Main Mall, Vancouver, British Columbia, V6T 1Z1, Canada.

<sup>2</sup>Department of Chemical and Biological Engineering, The University of British Columbia, 2360 East Mall, Vancouver, British Columbia, V6T 1Z3, Canada.

<sup>3</sup>Stewart Blusson Quantum Matter Institute, The University of British Columbia, 2355 East Mall, Vancouver, British Columbia, V6T 1Z4, Canada.

<sup>4</sup>Canadian Institute for Advanced Research (CIFAR), 661 University Avenue, Toronto, Ontario, M5G 1M1, Canada.

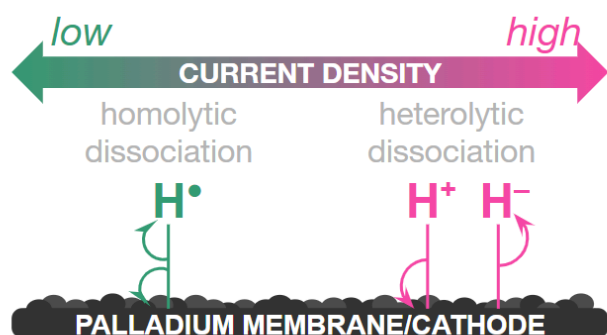
\*Corresponding author: Curtis P. Berlinguette

Email: [cberling@chem.ubc.ca](mailto:cberling@chem.ubc.ca)

## Abstract

Here, we use a palladium membrane reactor to investigate hydrogen transfer pathways at a palladium surface. The palladium membrane reactor uses electrochemistry to facilitate the controlled adsorption of hydrogen, sourced from water, into one face of a palladium foil. This hydrogen permeates through the palladium and reacts with unsaturated species in the opposing compartment. The amount of hydrogen loaded into the palladium can be controlled electrochemically to form a well-defined and static  $\text{PdH}_x$  ratio for studying chemical hydrogenation. These static  $\text{PdH}_x$  ratios are otherwise difficult to achieve. We show a preference for homolytic pathways at low current densities and heterolytic hydrogen transfer pathways at higher current densities. We also show reaction conditions that favor hydrogen reacting as either hydrogen radical ( $\text{H}^\bullet$ ), proton ( $\text{H}^+$ ), or hydride ( $\text{H}^-$ ).

## TOC



## Introduction

The hydrogenation of unsaturated species at a metal surface is performed at a massive scale across many industries.<sup>1</sup> Despite the significance of this chemistry to society, it is not always clear if hydrogenation proceeds through a heterolytic or homolytic pathway. This is because the identity of the reactive hydrogen species — hydrogen radical ( $\text{H}^\bullet$ ), proton ( $\text{H}^+$ ), or hydride ( $\text{H}^-$ ) — transferred to an unsaturated species at a metal surface is difficult to define.

Consider hydrogenation at a palladium surface using dihydrogen ( $\text{H}_2$ ) (Figure 1). After  $\text{H}_2$  binds to the surface, the H–H bond is broken and two Pd–H bonds are formed. If there is no change in metal oxidation state, this Pd–H species is broken homolytically to form  $\text{H}^\bullet$ .<sup>2</sup> However, palladium hydrogen systems are widely described as “palladium hydride”.<sup>3–7</sup> Neither of these descriptions contemplate a scenario where the hydrogen species reacts as  $\text{H}^+$ . This speaks to the challenges of accounting for hydrogen species and electrons, in addition to dihydrogen and substrate binding and liberation to and from a metal surface.<sup>2,8,8,9</sup>

We therefore sought a single platform that could accommodate, and control, homolytic and heterolytic hydrogenation pathways, thereby creating reactive hydrogen species at a palladium surface that could react as  $\text{H}^\bullet$ ,  $\text{H}^+$ , and  $\text{H}^-$ . To achieve this objective, we used a palladium membrane reactor to separate the adsorption of dihydrogen to a palladium surface from the transfer of the reactive hydrogen species to an unsaturated species. The palladium membrane reactor uses electrochemistry to produce a well-defined and static  $\text{PdH}_x$  ratio to study chemical hydrogenation.<sup>10</sup> This reactor also avoids the need to dissociate  $\text{H}_2$  at the same surface as hydrogenation (Figure 1). In contrast, thermochemical catalysis suffers from large changes in  $\text{PdH}_x$  ratios in response to small changes in temperature or pressure, and  $\text{H}_2$  dissociation occurs at the same surface as hydrogenation.<sup>11</sup>

Here, we show how the palladium membrane reactor mediates homolytic H transfer (where two Pd–H bonds are cleaved homolytically to generate two  $\text{H}^\bullet$ ) at lower current densities, and heterolytic H transfer (two Pd–H bonds are cleaved to form  $\text{H}^+$  and  $\text{H}^-$ ) at higher current densities. This outcome

enabled us to show the reaction conditions in which all of the reactive hydrogen species participate in hydrogenation chemistry. This platform also teaches how PdH<sub>x</sub> loading matters in these systems, providing an important complement to the rich literature studying reactive hydrogen species through Bronsted acids,<sup>12</sup> hydrogen transfer reagents,<sup>13</sup> and homogeneous catalysis.<sup>14</sup>

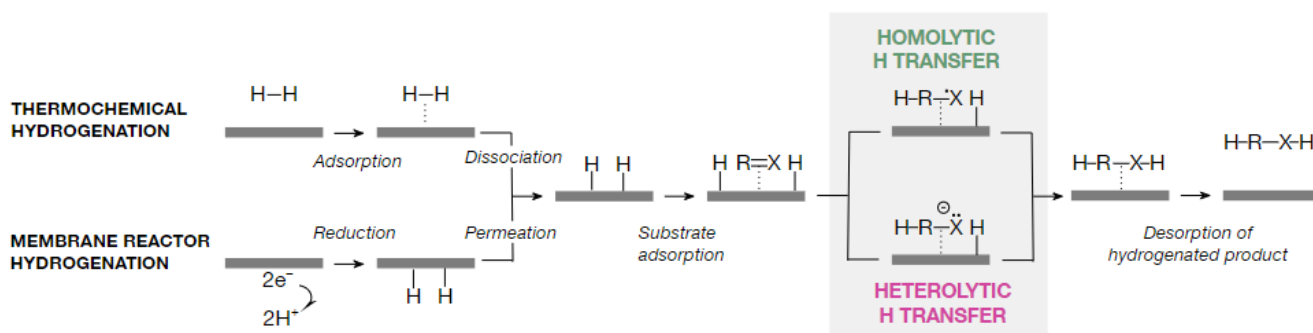


**Figure 1. Homolytic and Heterolytic hydrogen transfer pathways at Pd surfaces.** In thermochemical systems, H<sub>2</sub> adsorbs and dissociates onto a Pd surface (indicated by the grey rectangle). In the membrane reactor, an electrochemical potential reduces protons into adsorbed hydrogen atoms, which diffuse through the palladium membrane into an adjacent “hydrogenation chamber”. Once hydrogen atoms are positioned on Pd surface, they can react with a substrate through a homolytic pathway — where the Pd–H bond is cleaved homolytically to produce H•. These hydrogen atoms can also react through a heterolytic pathway — where two Pd–H bonds cleave asymmetrically to form a H<sup>+</sup> and a H<sup>-</sup>. The hydrogenated substrate can then desorb from the Pd surface. It is challenging to discern these two reaction pathways because both involve the net transfer of 2 protons and 2 electrons.

## Results

### *The palladium membrane reactor*

Palladium membrane reactors enable hydrogenation at ambient conditions, without the need for H<sub>2</sub>. The palladium membrane enables the protons that are generated by the electrolysis of water in the “electrolysis chamber” to be reduced to Pd–H on one face of a palladium foil. The adsorbed H atoms migrate through the hydrogen-permeable palladium to reach the opposing face of the palladium foil. This hydrogen is then poised to react with unsaturated species in the “hydrogenation chamber”.<sup>15–18</sup>

The palladium membrane reactor used in this study comprises two chambers physically separated by a dense sheet of Pd foil (Figure S1). These chambers are the electrochemical chamber and hydrogenation chamber, respectively. In the electrochemical chamber, protons are generated at an anode from the oxidation of a 1 M H<sub>2</sub>SO<sub>4</sub> solution. These protons migrate toward the palladium membrane that also serves as a cathode. Protons are reduced at the Pd surface to form surface adsorbed hydrogen atoms (H<sub>ads</sub>). H<sub>ads</sub> permeate the Pd cathode/membrane and emerge into the hydrogenation chamber, where they react with a substrate. Unless stated otherwise, the palladium membrane used in this study had an additional layer of Pd deposited onto the hydrogenation side to match the reaction conditions most often reported in the literature.<sup>15–17,19–21</sup> The anode in the electrochemical chamber was made of Pt mesh, and an Ag/AgCl reference electrode was used to monitor the cathodic potential for all experiments.

#### *Testing for hydrogen radicals (H•) formed through homolytic H-transfer*

Homolytic H-transfer pathways generate hydrogen radicals (H•) as the active hydrogen species. We used the stable radical 2,2,6,6,-tetramethylpiperidine-N-oxyl (TEMPO) as a chemical probe to trap hydrogen radicals generated at the Pd surface. Upon reaction with a hydrogen radical, TEMPO forms TEMPO–H (2,2,6,6,-tetramethylpiperidine-N-oxyl). Conveniently, TEMPO is red and TEMPO–H is not colored, which enabled us to track the reactions colorimetrically.<sup>22</sup>

We investigated homolytic Pd–H cleavage in the palladium membrane reactor containing 0.1 M TEMPO in ethanol in the hydrogenation chamber. Aliquots from the hydrogenation chamber were collected every hour of electrolysis and quantified using UV-vis spectroscopy, then qualified using GC–MS (Figures S2, S3).

We observed a reduction in [TEMPO] during electrolysis. The initial quenching rate of [TEMPO] was  $36 \pm 9$  mmol h<sup>-1</sup> (Figure 3, Figure S6). TEMPO was consumed until a concentration of  $18 \pm 3$  mM remained, at which point the system reached a steady state. We attribute this steady state to the TEMPO–H oxidation reaction that occurs readily in air. The mass spectrum of the product was 1

mass unit higher than the starting material, consistent with TEMPO reduction by  $\text{H}^\bullet$  to form TEMPO-H (Figure S3). Control experiments confirm that TEMPO is not reacting with the solvent or  $\text{H}_2$  (Figure S4).

We next sought to confirm that a concerted homolytic  $\text{H}^\bullet$  transfer pathway was reducing TEMPO and not a sequential  $\text{e}^-/\text{H}^+$  transfer pathway. We performed the same experiment using a copper foil in place of the palladium foil (Figure S5, S6). Because the copper foil conducts electrons, but is not permeable to hydrogen, any reaction with TEMPO has to proceed through direct electron transfer from the copper foil to form  $\text{TEMPO}^-$ , which is also colorless. If TEMPO were to unexpectedly react with  $\text{H}^+$ , then a direct electron transfer from copper would still be needed to form TEMPO-H. We did not observe any differences in  $[\text{TEMPO}]$  over 6 h of electrolysis with the copper membrane, despite the measured cathodic potential being much less than the reduction potential of TEMPO (Figure S5).

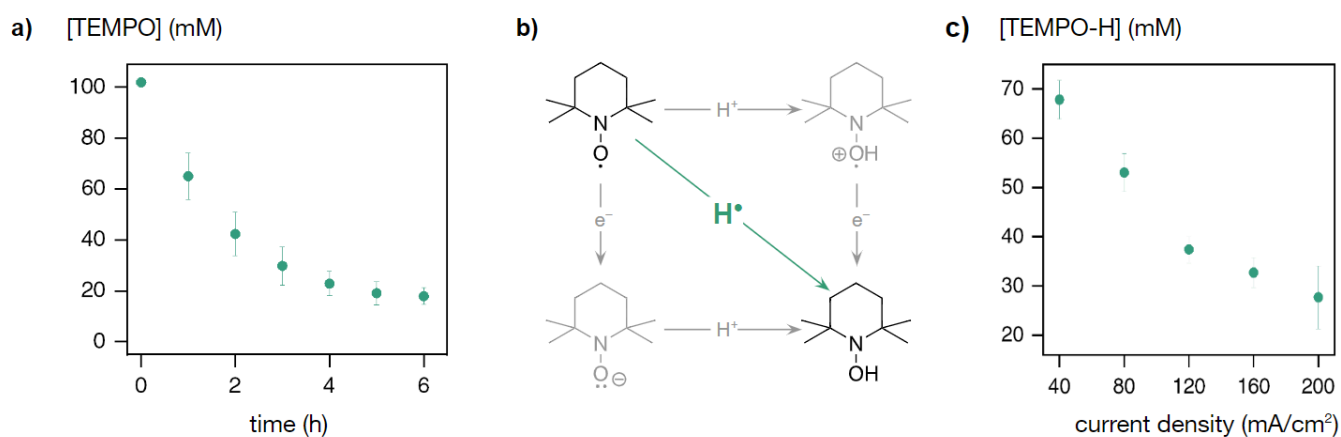
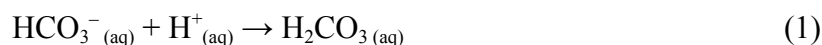


**Figure 2. TEMPO reduction in a palladium membrane reactor.** a) TEMPO concentration over time during the reaction of TEMPO with  $\text{H}^\bullet$  in a palladium membrane reactor at  $80 \text{ mA cm}^{-2}$ . Error bars are reported for triplicate experiments. b) Reaction scheme for the reduction of TEMPO to TEMPO-H by 1 proton and 1 electron. Pathways drawn in gray are not observed in our system. c) TEMPO-H concentration determined by UV-Vis spectroscopy after 1440 C of charge passed at 40, 80, 120, 160 and  $200 \text{ mA cm}^{-2}$ . As the current density increases the amount of TEMPO-H formed decreases. Error bars are reported for triplicate experiments.

### Testing for $H^+$ formed through heterolytic H-transfer

We previously demonstrated  $H^-$  as a reactive hydrogen species in a membrane reactor through the successful conversion of  $NAD^+$  to  $NADH$ .<sup>23</sup> While this result demonstrates a heterolytic hydrogen transfer pathway, we did not confirm the formation of  $H^+$ . Here, we designed our platform to detect  $H^+$  by using  $HCO_3^-$  as the reactant in the hydrogenation chamber. If  $H^+$  is the active reactive hydrogen species, then it should react with  $HCO_3^-$  to form  $H_2CO_3$  (Eq 1), which would then dissociate to form  $CO_{2(g)}$  (Eq 2). We do not expect that  $H^\bullet$  radicals and  $H^-$  would react with  $HCO_3^-$  to form  $CO_{2(g)}$ . We therefore used  $CO_{2(g)}$  as a chemical probe to detect protons.



An aqueous 1 M ammonium bicarbonate solution was placed in the hydrogenation chamber of the membrane reactor and sparged with  $N_2$  gas for 18 h prior to any experiment. The gas outlet of the hydrogenation chamber was connected to a gas chromatograph (GC). All other openings in the hydrogenation chamber were sealed. Prior to applying any current to the reactor, and after 18 hours of  $N_2$  sparging, two data points were collected to establish a baseline  $CO_2$  signal. After these two data points were collected, a galvanostatic current density of  $120 \text{ mA cm}^{-2}$  was applied to the cell, and a datapoint was collected by GC every hour for 7 h of electrolysis (Figure S7).

We measured  $CO_2$  product in the headspace after initiating electrolysis. The amount of  $CO_2$  released reached a maximum within the first 4 h of reaction, then diminished. This experiment was repeated in triplicate for 4 h of reaction time, with samples taken every 0, 0.25, 1.5, 2.75, and 4 h of electrolysis (Figure 3). Hydrogen was the only other gaseous product detected.

To express these results, the baseline  $[CO_2]$  determined prior to electrolysis was subtracted from  $[CO_2]$  signal during electrolysis. We define this difference as  $\Delta CO_2$ . At 0.25 h of electrolysis, the  $\Delta CO_2$  was  $17 \pm 4$  ppm. The  $\Delta CO_2$  increased to  $30 \pm 6$  ppm at 1.5 h, then slowly decreased to  $5 \pm 4$  after 4 h.

The pH of the solution was measured before and after electrolysis (Figure S8). We observed that the pH decreased from 9.3 to 9.2 over 4 h of electrolysis. This pH change is significant considering the strong buffering capacity of  $\text{NH}_4\text{HCO}_3$ .

After 4 h of electrolysis, an aliquot of the reaction solution was sampled and analyzed by nuclear magnetic resonance (NMR) to confirm formate was produced (Figure S9). This result was consistent with the hydrogenation of  $\text{CO}_2$ .<sup>10</sup>

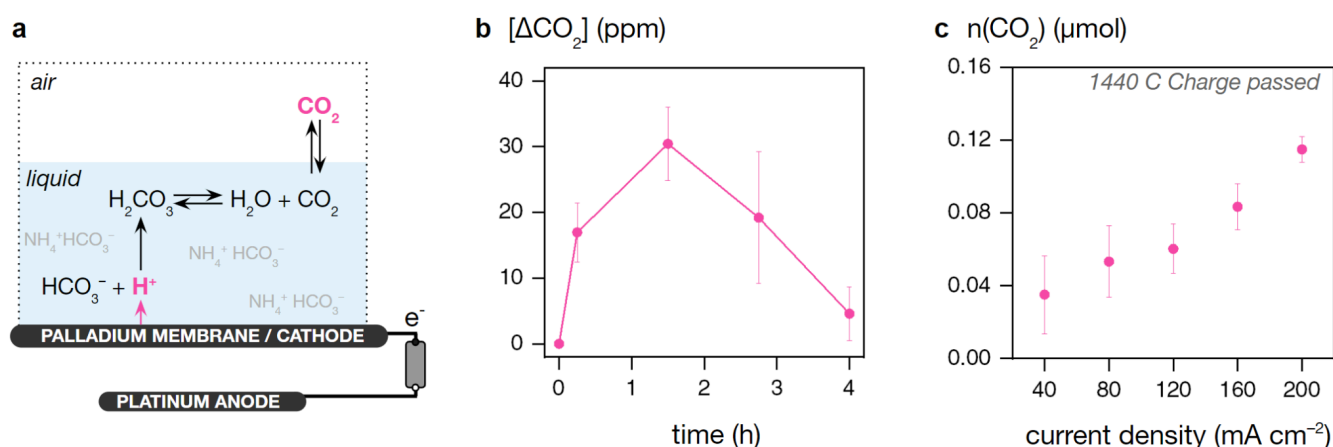


**Figure 3. Reaction of  $\text{NH}_4\text{HCO}_3$  in a palladium membrane reactor.** a) Schematic of the chemical reactions involved in producing  $\text{CO}_2$  from  $\text{NH}_4\text{HCO}_3$  solution. b)  $\Delta\text{CO}_2$  over time during the reaction of  $\text{NH}_4\text{HCO}_3$  in the palladium membrane reactor at  $120 \text{ mA cm}^{-2}$ . Error bars are reported for triplicate experiments. c) Moles of  $\text{CO}_2$  ( $n(\text{CO}_2)$ ) measured at current densities of 40, 80, 120, 160 and  $200 \text{ mA cm}^{-2}$ .  $n(\text{CO}_2)$  was calculated by integrating the area under the  $\Delta\text{CO}_2$  vs. time curve at a time point equivalent to 1440 C of charge passed through the reactor. Error bars are reported for triplicate experiments.

### Comparing how polarization affects the hydrogenation pathways

The H:Pd ratio ( $x$ ) of a palladium membrane can be increased by increasing the current density. For example, the ratio can increase from 0.8 to 0.85 when the current density is increased from 25 to 250  $\text{mA cm}^{-2}$ .<sup>10</sup> We therefore tested how the polarization of the palladium membrane affected different hydrogenation pathways. A galvanostatic current (40, 80, 120, 160, or 200  $\text{mA cm}^{-2}$ ) was applied to the membrane, while a cathodic potential was recorded using an Ag/AgCl reference electrode (Table S2). We added a 0.1 M solution of TEMPO in ethanol or a 1 M solution of  $\text{NH}_4\text{HCO}_3$  to the hydrogenation chamber to test for the homolytic and heterolytic H transfer pathways, respectively. The total amount of TEMPO-H and  $\text{CO}_2$  produced was recorded after a total charge of 1440 C had passed (corresponding to 4, 2, 1.33, 1, and 0.8 h of reaction at 40, 80, 120, 160, or 200  $\text{mA cm}^{-2}$ , respectively; Figures 2 and 3).

These experiments revealed a preference for TEMPO reduction at lower current densities and a preference for  $\text{CO}_2$  production at higher current densities (Figure 4, Figure S10). As the applied current density increased from 40 to 200  $\text{mA cm}^{-2}$ , TEMPO-H production decreased from  $68 \pm 4$  to  $28 \pm 6$  mmol, while the amount of  $\text{CO}_2$  increased from  $0.035 \pm 0.021$  to  $0.114 \pm 0.007$   $\mu\text{mol}$  (Figure 4).

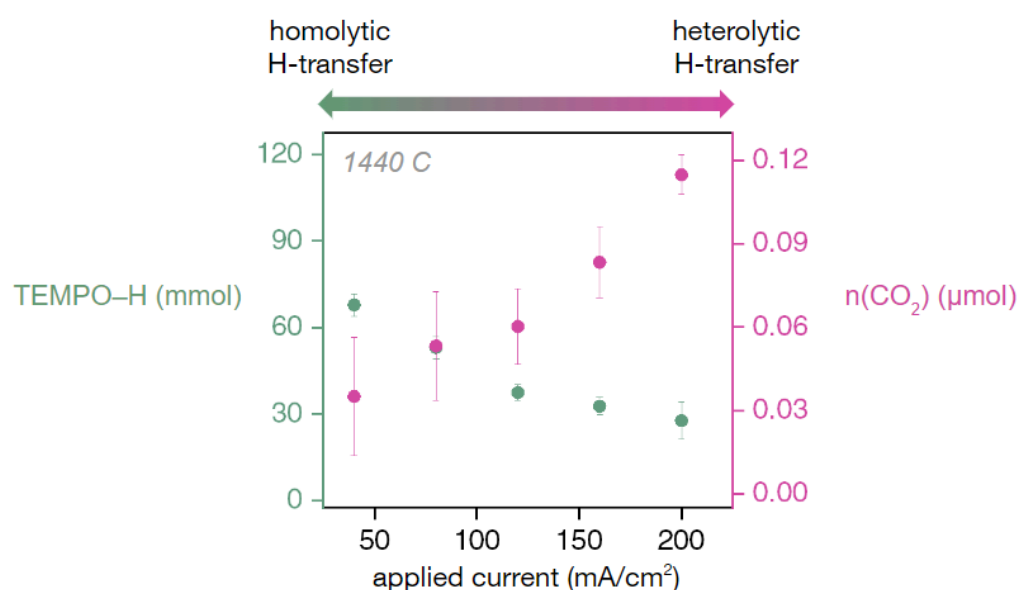


**Figure 4. Comparison of polarization effects on TEMPO–H and CO<sub>2</sub> formation.** All data is presented for a reaction with a constant charge of 1440 C. The left axis shows the amount of TEMPO–H formed when TEMPO was used as a reactant in the palladium membrane reactor. The right axis shows the total amount of CO<sub>2(g)</sub> measured when NH<sub>4</sub>HCO<sub>3</sub> was used as a reactant. Error bars are reported for triplicate experiments.

## Discussion

In thermochemical systems, hydrogen can be transferred from a heterogeneous metal surface to a reactant in solution as: (1) a radical (H•), through a homogeneous mechanism; or 2) a proton (H<sup>+</sup>) and hydride (H<sup>-</sup>), through a heterogeneous mechanism.<sup>24</sup> The bond between hydrogen and late transition metals, like Pd, are considered to be covalent.<sup>25</sup> Hydrogen is therefore most often transferred to a reactant through a homolytic mechanism because of the minimal electronegativity difference between the two atoms.<sup>2</sup> To be observed, heterolytic mechanisms usually require catalyst surface modification such as oxides,<sup>26</sup> isolation of single atoms,<sup>27</sup> or a catalyst support<sup>28</sup>.

Electrochemical hydrogenation reactions follow the same concerted proton electron transfer pathway, but can also undergo direct electron transfer from an electrode surface to a reactant in solution.<sup>29,30</sup> This electron transfer is followed by a proton transfer (or vice versa) in a stepwise mechanism.<sup>31,32</sup> The type of reaction pathway depends on the reduction potential of the reactant, the electrode material, and the potential applied to the cathode. At very negative potentials, all mechanisms may occur simultaneously.<sup>33</sup>

The palladium membrane reactor is unique because it offers both thermochemical and electrochemical functionalities. The palladium membrane/cathode acts as: (i) a cathode; (ii) a hydrogen–selective membrane; and (iii) a heterogeneous hydrogenation catalyst. How thermochemical and electrochemical functionalities influence the reaction mechanism at the Pd surface has not been previously defined.

Consider the reactant scope of the palladium membrane reactor: non-polar (e.g. C=C),<sup>15–18,20,34–36</sup> weakly polar (e.g. C≡N),<sup>37</sup> and polar (e.g. C=O)<sup>21,38–40</sup> bonds have all been hydrogenated. Moreover,

other reactions like hydrodeoxygenation (cleavage of C–O bonds) and hydrodechlorination (cleavage of C–Cl bonds) have also been reported (Table S1).<sup>21,41–43</sup> This broad scope in reactivity is an indication that multiple hydrogen transfer mechanisms could be at play.

These observations prompted us to investigate the active hydrogen species in the palladium membrane reactor. Previous work by our group identified that hydride ( $H^-$ ) is generated at the palladium membrane surface; however, the goal of that study was to drive enzymatic catalysis cycles, not identify reaction mechanisms in the palladium membrane reactor.<sup>23</sup> Therefore, the field continues to lack experimental investigations into direct electron transfer mechanisms, homolytic reaction mechanisms, and proton formation in a heterolytic reaction mechanism.

To define the types of reaction mechanisms present in the palladium membrane reactor and to provide direct experimental evidence to support them, we first investigated if direct electron transfer from the palladium membrane to a reactant in the hydrogenation chamber was possible. Although the hydrogenation chamber is not under an electrochemical potential, the palladium membrane is still under an electric bias. Thus experimental confirmation of direct electron transfer mechanisms is required. Because it is challenging to decouple the movement of protons and electrons inside of the bulk Pd lattice, we turned to a hydrogen impermeable Cu membrane to isolate the movement of electrons in this system.<sup>44</sup> Under the assumption that TEMPO adsorbs to both Pd and Cu: if direct electron transfer is possible from the bulk metal membrane/cathode to a reactant in the hydrogenation chamber, we should observe it using a Cu membrane. TEMPO was chosen as a chemical probe for direct electron transfer from the membrane/cathode because it can be reduced by 1 electron and is redox active. We observed no TEMPO reduction when a Cu membrane was used, however TEMPO was reduced when a palladium membrane was used (Figure S5).

Based on this result, we concluded that TEMPO was reduced by hydrogen atoms ( $H^\bullet$ ) that permeated through the palladium membrane. We further validated this claim by using a palladium membrane coated Pd black to mimic the reaction conditions most often reported in the literature.<sup>16,20,21,45</sup>

The addition of the Pd black accelerated the rate of TEMPO reduction 1.4-fold (Figure S6). Within the first hour of electrolysis, TEMPO was reduced at a rate of 38 mM h<sup>-1</sup>. The rate of TEMPO reduction decreased to 1 mM h<sup>-1</sup> after 6 h of reaction, and the TEMPO concentration remained at 18 mM (Figure 2). We attribute this decrease in reaction rate to an equilibrium between the reduction and oxidation reaction (from the ambient air) being established.<sup>46</sup> GC-MS spectra confirmed TEMPO-H was the only reaction product (Figure S3). The reduction of TEMPO to TEMPO-H confirmed the formation of H• at the palladium membrane surface. The formation of these hydrogen species aligns with a homolytic Pd-H cleavage and hydrogenation mechanism.

We next evaluated heterolytic hydrogen desorption mechanisms in the palladium membrane reactor. Heterolytic hydrogen transfer mechanisms invoke water-assisted charge separation (Figure S11).<sup>23,47</sup> This theory suggests that solvent (i.e. water) can act as both a Lewis acid or base to facilitate heterogeneous Pd-H cleavage. This theory also assumes H<sup>+</sup> and H<sup>-</sup> occur simultaneously. Since hydrides (H<sup>-</sup>) have already been detected in a previous work,<sup>23</sup> we focused on detecting protons (H<sup>+</sup>).

The experimental resolution of H<sup>+</sup> from H<sup>-</sup> at a palladium surface is nontrivial. If we used a Lewis base to trap H<sup>+</sup>, then the product (conjugate acid) could react with H<sup>-</sup> to produce H<sub>2</sub>. Conversely, if we used a Lewis acid to trap H<sup>-</sup>, the conjugate base could react with H<sup>+</sup> to produce H<sub>2</sub>. We therefore used HCO<sub>3</sub><sup>-</sup> as a H<sup>+</sup> trap, because the product releases gaseous CO<sub>2</sub>, thus is physically separated from the reaction (Figure 3).

When no current was passed through the palladium membrane reactor, we consistently detected 78 ppm of CO<sub>2</sub>. When the cell was turned on, the concentration of CO<sub>2</sub> spiked to 105 ppm, then slowly decreased to 90 after 4 h of reaction. When we triplicated this study, we found the maximum ΔCO<sub>2</sub> detected was 30 ± 6 ppm. We attribute this spike in CO<sub>2</sub> production to the reaction of HCO<sub>3</sub><sup>-</sup> with H<sup>+</sup>. The formation of the H<sub>2</sub>CO<sub>3</sub> intermediate is confirmed by a 0.1 decrease in pH of the bulk solution, which is significant considering the strong buffering capacity of NH<sub>4</sub>HCO<sub>3</sub> (Figure S8). At pH ~9, the NH<sub>4</sub>HCO<sub>3</sub> buffer has a pK<sub>a</sub> of 9.2.<sup>48</sup> If it is assumed that the concentration of base in the system remains

constant, then the concentration of acid in the solution would have to increase by 1.25-fold to drive this observed pH change according to the Henderson Hasselbalch equation. These results are a good indication that protons are being liberated from the Pd membrane surface.

Finally, we conducted a qualitative investigation on the effect of Pd polarization on the proton electron transfer mechanism using the above two model reactions. We note that since we investigated two different reactions, our results do not reflect quantitative information that links the polarization to the type of reaction mechanism, hence the different y-axis scales in Figure 4. These results, however, provide a qualitative basis for future investigation into controlled reaction mechanisms in a palladium membrane reactor. We investigated current densities of 40, 80, 120, 160, and 200 mA cm<sup>-2</sup> and found the rate of H<sup>•</sup> transfer decreased with increasing current density, while the rate of H<sup>+</sup> transfer increased with increasing current density (Figure 4). We observe a similar trend when these results are plotted against the cathodic potential (Figure S10). This result aligns with studies on the polarization-dependence of H<sup>-</sup> transfer on electrodes, where higher degrees of polarization result in greater thermodynamic hydricities of H<sup>-</sup>.<sup>49</sup> Moreover, previously studied reactions in the palladium membrane reactor hypothesized to involve a H<sup>+</sup>/H<sup>-</sup> transfer (e.g. the hydrodeoxygenation of furfuryl alcohol to methyltetrahydrofuran)<sup>21</sup> were only favorable at current densities >175 mA cm<sup>-2</sup>.

## Conclusion

This study defines the possible types of hydrogen transfer pathways on heterogeneous Pd surfaces. Building on previous work, we establish reactive hydrogen species can be a hydrogen atom (H<sup>•</sup>), proton (H<sup>+</sup>), or hydride (H<sup>-</sup>). We further demonstrate a qualitative relationship between electrode polarization and hydrogen transfer mechanism. Specifically, higher degrees of electrode polarization favor a heterolytic hydrogen transfer mechanism (i.e. H<sup>+</sup>/H<sup>-</sup>), while lower degrees favor a homolytic hydrogen transfer mechanism (H<sup>•</sup>). This work fills a fundamental gap in palladium membrane reactor

literature and invites further investigation into the chemical scope and reactivity of the palladium membrane reactor.

## **Author Information**

### **Corresponding author**

Curtis P. Berlinguette – Department of Chemistry, The University of British Columbia, 2036 Main Mall, Vancouver, British Columbia, V6T 1Z1, Canada; Department of Chemical and Biological Engineering, The University of British Columbia, 2360 East Mall, Vancouver, British Columbia, V6T 1Z3, Canada; Stewart Blusson Quantum Matter Institute, The University of British Columbia, 2355 East Mall, Vancouver, British Columbia, V6T 1Z4, Canada; Canadian Institute for Advanced Research (CIFAR), 661 University Avenue, Toronto, Ontario, M5G 1M1, Canada; Email: [cberling@chem.ubc.ca](mailto:cberling@chem.ubc.ca)

### **Competing interests**

Patent applications based on the palladium membrane reactor technology described in this work have been filed (one has been granted): Berlinguette, C. P.; Sherbo, R. S. “Methods and Apparatus for Performing Chemical and Electrochemical Reactions”. Canadian Patent Application No. 3089508, Publication No. CA3089508 (published August 2019), pending. US Patent No. US11667592B2, granted June 2023. US Patent Application No. 18/305,970, Publication No. US20230257325A1 (published August 2023), pending. Priority data: US Provisional Patent Application No. 62/622,305, filed January 2018. The remaining authors declare no other competing interests.

### **Acknowledgements**

The authors would like to thank Dr. Monika Stolar (UBC Vancouver) for valuable scientific discussion. The authors are grateful to the Natural Sciences and Engineering Research Council of Canada (RGPIN-2024-06486), Canada Foundation for Innovation (229288), Canadian Institute for Advanced Research (BSE-BERL-162173), and Canada Research Chairs for financial support. This research was undertaken thanks in part to funding from the Canada First Research Excellence Fund, Quantum Materials and Future Technologies Program.

## References

- (1) Roessler, F. Catalysis in the Industrial Production of Pharmaceuticals and Fine Chemicals. *CHIMIA International Journal for Chemistry* **1996**, *50* (3), 106–109.
- (2) Horiuti, I.; Polanyi, M. Exchange Reactions of Hydrogen on Metallic Catalysts. *Trans. Faraday Soc.* **1934**, *30* (0), 1164–1172.
- (3) Lewis, F. A. The Hydrides of Palladium and Palladium Alloys. *Platin. Met. Rev.* **1960**, *4* (4), 132–137.
- (4) Yang, X.; Li, H.; Ahuja, R.; Kang, T.; Luo, W. Formation and Electronic Properties of Palladium Hydrides and Palladium-Rhodium Dihydride Alloys under Pressure. *Sci. Rep.* **2017**, *7* (1), 3520.
- (5) Gdowski, G. E.; Felner, T. E.; Stulen, R. H. Effect of Surface Temperature on the Sorption of Hydrogen by Pd(111). *Surf. Sci.* **1987**, *181* (3), L147–L155.
- (6) Duś, R.; Nowicka, E. Hydrogen Segregation on a Palladium Hydride Surface. *Prog. Surf. Sci.* **1998**, *59* (1-4), 289–300.
- (7) Setayandeh, S. S.; Webb, C. J.; Gray, E. M. Electron and Phonon Band Structures of Palladium and Palladium Hydride: A Review. *Prog. Solid State Chem.* **2020**, *60*, 100285.
- (8) Fonocho, R.; Gardner, C. L.; Ternan, M. A Study of the Electrochemical Hydrogenation of O-Xylene in a PEM Hydrogenation Reactor. *Electrochim. Acta* **2012**, *75*, 171–178.
- (9) Jenkins, G. I.; Rideal, E. The Catalytic Hydrogenation of Ethylene at a Nickel Surface. Part II. The Reaction Mechanism. *J. Chem. Soc.* **1955**, No. 0, 2496–2500.
- (10) Hunt, C.; Kurimoto, A.; Wood, G.; LeSage, N.; Peterson, M.; Luginbuhl, B. R.; Horner, O.; Issinski, S.; Berlinguette, C. P. Endergonic Hydrogenation at Ambient Conditions Using an Electrochemical Membrane Reactor. *J. Am. Chem. Soc.* **2023**, *145* (26), 14316–14323.
- (11) Wicke, E.; Brodowsky, H.; Züchner, H. Hydrogen in Palladium and Palladium Alloys. In *Hydrogen in Metals II: Application-Oriented Properties*; Alefeld, G., Völkl, J., Eds.; Springer Berlin Heidelberg: Berlin, Heidelberg, 1978; pp 73–155.
- (12) Reijenga, J.; van Hoof, A.; van Loon, A.; Teunissen, B. Development of Methods for the Determination of pK<sub>a</sub> values. *Anal. Chem. Insights* **2013**, *8*, ACI.S12304.
- (13) Agarwal, R. G.; Coste, S. C.; Groff, B. D.; Heuer, A. M.; Noh, H.; Parada, G. A.; Wise, C. F.; Nichols, E. M.; Warren, J. J.; Mayer, J. M. Free Energies of Proton-Coupled Electron Transfer Reagents and Their Applications. *Chem. Rev.* **2022**, *122* (1), 1–49.
- (14) Fukuzumi, S.; Yamada, Y.; Suenobu, T.; Ohkubo, K.; Kotani, H. Catalytic Mechanisms of Hydrogen Evolution with Homogeneous and Heterogeneous Catalysts. *Energy Environ. Sci.* **2011**, *4* (8), 2754–2766.
- (15) Iwakura, C.; Yoshida, Y.; Ogata, S.; Inoue, H. New Hydrogenation Systems of Unsaturated Organic Compounds Using Noble Metal-Deposited Palladium Sheet Electrodes with Three-Dimensional Structures. *J. Mater. Res.* **1998**, *13* (4), 821–824.
- (16) Sherbo, R. S.; Delima, R. S.; Chiykowski, V. A.; MacLeod, B. P.; Berlinguette, C. P. Complete Electron Economy by Pairing Electrolysis with Hydrogenation. *Nature Catalysis* **2018**, *1* (7), 501–507.
- (17) Sherbo, R. S.; Kurimoto, A.; Brown, C. M.; Berlinguette, C. P. Efficient Electrocatalytic Hydrogenation with a Palladium Membrane Reactor. *J. Am. Chem. Soc.* **2019**, *141* (19), 7815–7821.
- (18) Inoue, H.; Abe, T.; Iwakura, C. Successive Hydrogenation of Styrene at a Palladium Sheet Electrode Combined with Electrochemical Supply of Hydrogen. *Chem. Commun.* **1996**, No. 1, 55–56.
- (19) Iwakura, C.; Yoshida, Y.; Inoue, H. A New Hydrogenation System of 4-Methylstyrene Using a Palladinized Palladium Sheet Electrode. *J. Electroanal. Chem.* **1997**, *431* (1), 43–45.
- (20) Jansonius, R. P.; Kurimoto, A.; Marelli, A. M.; Huang, A.; Sherbo, R. S.; Berlinguette, C. P. Hydrogenation without H<sub>2</sub> Using a Palladium Membrane Flow Cell. *Cell Reports Physical Science* **2020**, *1* (7), 100105.
- (21) Stankovic, M. D.; Sperry, J. F.; Delima, R. S.; Rupnow, C. C.; Rooney, M. B.; Stolar, M.; Berlinguette, C. P. Electrochemical Production of Methyltetrahydrofuran, a Biofuel for Diesel Engines. *Energy Environ. Sci.* **2023**, *16* (8), 3453–3461.
- (22) Gerken, J. B.; Stahl, S. S. High-Potential Electrocatalytic O<sub>2</sub> Reduction with nitroxyl/NO X Mediators: Implications for Fuel Cells and Aerobic Oxidation Catalysis. *ACS Cent. Sci.* **2015**, *1* (5), 234–243.
- (23) Kurimoto, A.; Nasser, S. A.; Hunt, C.; Rooney, M.; Dvorak, D. J.; LeSage, N. E.; Jansonius, R. P.; Withers, S. G.; Berlinguette, C. P. Bioelectrocatalysis with a Palladium Membrane Reactor. *Nat. Commun.* **2023**, *14* (1), 1814.

- (24) Aireddy, D. R.; Ding, K. Heterolytic Dissociation of H<sub>2</sub> in Heterogeneous Catalysis. *ACS Catal.* **2022**, *12* (8), 4707–4723.
- (25) Hammer, B.; Nørskov, J. K. Electronic Factors Determining the Reactivity of Metal Surfaces. *Surf. Sci.* **1995**, *343* (3), 211–220.
- (26) Coluccia, S.; Boccuzzi, F.; Ghiotti, G.; Mirra, C. Evidence for Heterolytic Dissociation of H<sub>2</sub> on the Surface of Thermally Activated MgO Powders. *Zeitschrift für Physikalische Chemie* **1980**, *121* (1), 141–143.
- (27) Lu, J.; Aydin, C.; Browning, N. D.; Gates, B. C. Hydrogen Activation and Metal Hydride Formation Trigger Cluster Formation from Supported Iridium Complexes. *J. Am. Chem. Soc.* **2012**, *134* (11), 5022–5025.
- (28) Fujitani, T.; Nakamura, I.; Akita, T.; Okumura, M.; Haruta, M. Hydrogen Dissociation by Gold Clusters. *Angew. Chem. Int. Ed Engl.* **2009**, *48* (50), 9515–9518.
- (29) Zhang, S.; Findlater, M. Electrochemically Driven Hydrogen Atom Transfer Catalysis: A Tool for C(sp<sup>3</sup>)/Si-H Functionalization and Hydrofunctionalization of Alkenes. *ACS Catal.* **2023**, *13* (13), 8731–8751.
- (30) Hickey, D. P.; Minter, S. D. Coupling Theory to Electrode Design for Electrocatalysis. *ACS Cent Sci* **2019**, *5* (5), 745–746.
- (31) de Hemptinne, X.; Jüngers, J. C. Sur Le Mécanisme de L'hydrogénation électrochimique. *Zeitschrift für Physikalische Chemie* **1958**, *15* (1-6), 137–148.
- (32) Wagner, C. Considerations on the Mechanism of the Hydrogenation of Organic Compounds in Aqueous Solutions on Noble Metal Catalysts. *Electrochim. Acta* **1970**, *15* (6), 987–997.
- (33) Moutet, J.-C. ELECTROCATALYTIC HYDROGENATION ON HYDROGEN-ACTIVE ELECTRODES. A REVIEW. *Org. Prep. Proced. Int.* **1992**, *24* (3), 309–325.
- (34) Delima, R. S.; Sherbo, R. S.; Dvorak, D. J.; Kurimoto, A.; Berlinguette, C. P. Supported Palladium Membrane Reactor Architecture for Electrocatalytic Hydrogenation. *J. Mater. Chem. A Mater. Energy Sustain.* **2019**, *7* (46), 26586–26595.
- (35) Yan, Y.-Q.; Wei, Z.; Wang, Z.; Li, Y.; Wang, W.-H.; Jiang, B.; Su, B.-L. H<sub>2</sub>-Free Semi-Hydrogenation of Butadiene by the Atomic Sieving Effect of Pd Membrane with Tree-like Pd Dendrites Array. *Angew. Chem. Int. Ed Engl.* **2023**, *62* (38), e202309013.
- (36) Yan, Y.-Q.; Chen, Y.; Wang, Z.; Chen, L.-H.; Tang, H.-L.; Su, B.-L. Electrochemistry-Assisted Selective Butadiene Hydrogenation with Water. *Nat. Commun.* **2023**, *14* (1), 2106.
- (37) Zhang, Y.; Kornienko, N. C≡N Triple Bond Cleavage via Transmembrane Hydrogenation. *Chem Catalysis* **2022**, *2* (3), 499–507.
- (38) Inoue, H.; Ito, T.; Iwakura, C. Control of Product Distribution in the Hydrogenation of Crotonaldehyde, Butyraldehyde and Crotyl Alcohol Using the Successive Hydrogenation System. *Electrochemistry* **2001**, *69* (9), 699–701.
- (39) Huang, A.; Cao, Y.; Delima, R. S.; Ji, T.; Jansonius, R. P.; Johnson, N. J. J.; Hunt, C.; He, J.; Kurimoto, A.; Zhang, Z.; Berlinguette, C. P. Electrolysis Can Be Used to Resolve Hydrogenation Pathways at Palladium Surfaces in a Membrane Reactor. *JACS Au* **2021**, *1* (3), 336–343.
- (40) Delima, R. S.; Stankovic, M. D.; MacLeod, B. P.; Fink, A. G.; Rooney, M. B.; Huang, A.; Jansonius, R. P.; Dvorak, D. J.; Berlinguette, C. P. Selective Hydrogenation of Furfural Using a Membrane Reactor. *Energy Environ. Sci.* **2021**. <https://doi.org/10.1039/D1EE02818A>.
- (41) Nieto-Sandoval, J.; Gomez-Herrero, E.; Munoz, M.; de Pedro, Z. M.; Casas, J. A. Palladium-Based Catalytic Membrane Reactor for the Continuous Flow Hydrodechlorination of Chlorinated Micropollutants. *Appl. Catal. B* **2021**, *293*, 120235.
- (42) del Olmo, R. B.; Torres, M.; Nieto-Sandoval, J.; Munoz, M.; de Pedro, Z. M.; Casas, J. A. Precious Metal-Based Catalytic Membrane Reactors for Continuous Flow Catalytic Hydrodechlorination. *Journal of Environmental Chemical Engineering* **2024**, *12* (3), 112754.
- (43) Inoue, H.; Higashiyama, K.; Higuchi, E.; Iwakura, C. A Dechlorination System for 4-Chlorotoluene Using a Two-Compartment Cell Separated by a Palladized Ion Exchange Membrane. *J. Electroanal. Chem.* **2003**, *560* (1), 87–91.
- (44) McLellan, R. B.; Harkins, C. G. Hydrogen Interactions with Metals. *Mater. Sci. Eng.* **1975**, *18* (1), 5–35.
- (45) Inoue, H.; Yoshida, Y.; Ogata, S.; Shimamune, T.; Iwakura, C. Effect of Pd Black Deposits on Successive Hydrogenation of 4-Methylstyrene with Active Hydrogen Passing Through a Pd Sheet Electrode. *J. Electrochem. Soc.* **1998**, *145* (1), 138.
- (46) Zhao, X.; Yang, J.-D.; Cheng, J.-P. Revisiting the Electrochemistry of TEMPOH Analogues in Acetonitrile.

*J. Org. Chem.* **2023**, 88 (1), 540–547.

- (47) Zhao, Z.; Bababrik, R.; Xue, W.; Li, Y.; Briggs, N. M.; Nguyen, D.-T.; Nguyen, U.; Crossley, S. P.; Wang, S.; Wang, B.; Resasco, D. E. Solvent-Mediated Charge Separation Drives Alternative Hydrogenation Path of Furanics in Liquid Water. *Nature Catalysis* **2019**, 2 (5), 431–436.
- (48) Waters corporation. Mobile Phase Chart. 2023.  
<https://www.waters.com/webassets/cms/library/docs/720002117en.pdf>.
- (49) Wang, H.-X.; Toh, W. L.; Tang, B. Y.; Surendranath, Y. Metal Surfaces Catalyze Polarization-Dependent Hydride Transfer from H<sub>2</sub>. *Nature Catalysis* **2023**, 6 (4), 351–362.